

# Direct and Independent Estimation of $B_0$ Components based on Raw EPI Data

F. Testud<sup>1</sup>, I. Dragonu<sup>1</sup>, J. Hennig<sup>1</sup>, and M. Zaitsev<sup>1</sup>

<sup>1</sup>Medical Physics, Department of Diagnostic Radiology, University Hospital Freiburg, Freiburg, Germany

**Introduction:** Gradient Recalled Echo Planar Imaging (GRE-EPI) is sensitive to spatial and temporal changes of  $B_0$  arising from susceptibility effects, temperature changes of the shims and motion of the subject. This leads to time variation of image artifacts such as distortions and intensity losses. Commonly, distortion correction is performed based on a calibration scan preceding the actual measurements so temporal changes of  $B_0$  can not be taken into account. A possible remedy is the extraction of field gradients from EPI raw data as published [1, 2, 3] (method A, B and C respectively). For all three methods, the gradient maps in readout direction ( $G_x$ ) are however dependent on the gradient maps in phase encoding direction ( $G_y$ ). Here a novel filter scheme to estimate  $G_x$ -maps independently from  $G_y$ -maps is presented. The gradient maps calculated with the method introduced here are compared with A, B and C in in-vivo experiments.

$$\mathcal{J}_f(\vec{r}, p_{k_y}) = \mathcal{F}T^{-1} \left\{ S(\vec{k}) \right\} \otimes \mathcal{F}T^{-1} \left\{ f(\vec{k}, p_{k_y}, p_{k_x}, \sigma_{k_y}, \sigma_{k_x}) \right\} \quad (\text{Eq. 1})$$

**Theory:** The  $k$ -space filtering concept [3] can be formulated as a convolution between the signal  $S$  and a sliding filter  $f$  centered at  $(p_{k_x}, p_{k_y})$  and with optimized widths  $\sigma_x$  and  $\sigma_y$ . (Eq. 1) can be separated of  $x$  and  $y$  which allows to perform two filter operations in hybrid spaces. A 2D wave with Gaussian shape is used as filter  $f$ . The position of the maximum of  $\mathcal{J}_f$  (Eq. 1) is proportional to the echo shifts  $\delta_{k_y}$  and  $\delta_{k_x}$  which are calculated for each pixel. The gradient maps are calculated with (Eq. 2).  $\Delta_T$  is the echo spacing time,  $t_{TE}$  the echo time and  $\Delta_{k_y}$  the  $k$ -space pixel size. As seen in (Eq. 2) the fraction in  $G_x$  is the tangents of the angle  $\Theta$  in the triangle OPA (Fig. 1 a) which describes the contour line for  $G_x$  (see Fig. 1a) in case of a Cartesian trajectory and when the dwell is neglected. In order to have good matching between the sliding filter and the contour lines for  $G_x$  estimation, the trajectory of the sliding filter has to match the contour line. This method, referred to as D, is shearing  $f$  by  $\Theta$  with fixed point O.  $G_x$ -maps can be estimated directly from the angle  $\Theta$  at which the pixel intensity is maximal (Eq. 1 & 3).  $G_y$ -maps are determined in the same manner as in C.

$$G_y = \frac{\delta_{k_y}}{\gamma \left( t_{TE} + \delta_{k_y} \frac{\Delta_T}{\Delta_{k_y}} \right)}, \quad G_x = \frac{\delta_{k_x}}{\gamma \left( t_{TE} + \delta_{k_y} \frac{\Delta_T}{\Delta_{k_y}} \right)} \quad (\text{Eq. 2})$$

$$G_x = \frac{\tan(\Theta)}{\gamma} \quad (\text{Eq. 3})$$

**Methods:** One experiment was performed on a 3T Tim TRIO scanner (Siemens Healthcare, Erlangen, Germany). Echo planar (EP), gradient echo image reconstruction and the methods A, B, C and D were implemented in MATLAB (The Mathworks, Natick, AM, USA).  $B_0$  maps of 40 slices from six healthy volunteers were measured with a dual echo GRE sequence ( $t_{TE1}=3.78\text{ms}$ ,  $t_{TE2}=6.24\text{ms}$ ,  $t_{TR}=345\text{ms}$ ,  $\text{FOV}=240 \times 240 \times 2.5\text{mm}$ , matrix size  $96 \times 96$ ) and corresponding EP images ( $t_{TE}=33\text{ms}$ ,  $\Delta_T=0.6\mu\text{s}$ ) were acquired. Images were masked and co-registered with FSL[4]. The  $B_0$  maps were used to distort the dual GRE images and simulate distorted field maps  $B_{D0}$ . The gradients maps of  $B_{D0}$  and from the 4 methods were calculated. The root mean square deviation (RMSD) between the gradient maps from  $B_{D0}$  and A, B, C and D was calculated and averaged (aRMSD) over the number of volunteers and slices. Slices with large amount of signal losses resulting in incorrect masking were omitted from averaging.

**Results:** The results are summarized in Fig. 2. It is visible that the methods D and C have similar and lower aRMSD compared to the methods B and A. In Fig. 3  $G_x$  maps from the A, B, C, D and from  $B_{D0}$  are shown. The methods D and C give visually identical  $G_x$  maps which are smoother than the maps from A and B.

**Conclusion:** In this work we show that the proposed filter scheme (D) produce  $G_x$  and  $G_y$  maps which are more accurate than B and A and equally precise as C. The proposed filter scheme has the advantage of estimating  $G_x$  maps independently from  $G_y$  values. The presented method is using the contour lines to calculate  $G_x$  and  $G_y$ . The contour lines are specific for a given  $k$ -space trajectory (here Cartesian). For a given trajectory the contour lines have to be derived in order to design an appropriate sliding filter scheme. Fig 1 b) is illustrating the contour lines of  $G_x$  in case of a spiral trajectory.

**Acknowledgments:** This work has been supported by the German Research Foundation, grants SP 632/3 – 1 and ZA 422/2 – 1 in part by the INUMAC project supported by the German Federal Ministry of Education and Research, grant #01EQ0605.

**References:**[1] R Deichmann et al., NI 15, 2002, [2] N Chen et al., NI 31, 2006,

[3] F Testud et al., Joint Annual Meeting ISMRM-ESMRMB, p368 (2007), [4] S M Smith et al., NI 23, 2004

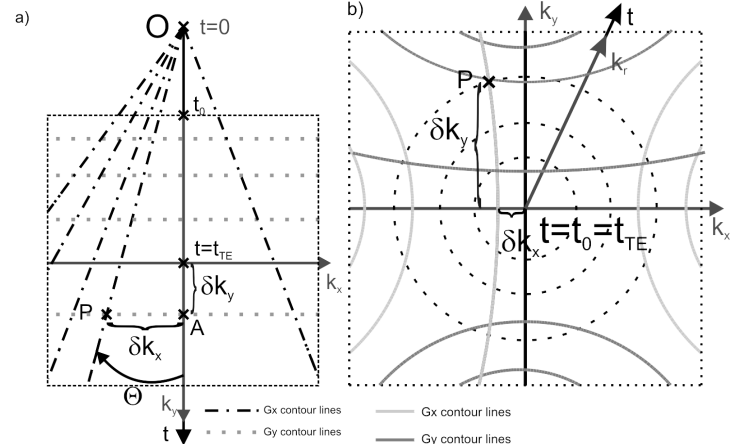


Fig 1 a): Illustration of the  $G_x$  (dash dotted line) and  $G_y$  (dotted line) contour lines, in  $k_x$ - $t$  space.  $t_0$  is the time between the RF pulse and the  $k$ -space acquisition start.  $P$  is the echo and  $A$  its projection on the  $t$ -( $k_y$ ) axis.  $k$ -space is delimited by a dotted square. b): Illustration of the contour lines for a spiral trajectory. The dotted line is the spiral when the azimuth time can be neglected. Top and bottom are the  $G_y$  contour lines and right and left the  $G_x$  contour lines.

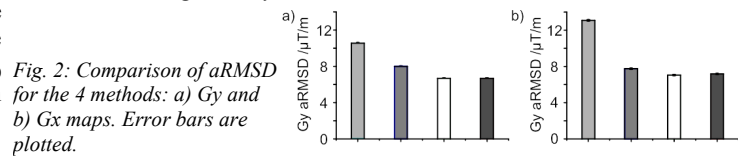


Fig. 2: Comparison of aRMSD for the 4 methods: a)  $G_y$  and b)  $G_x$  maps. Error bars are plotted.

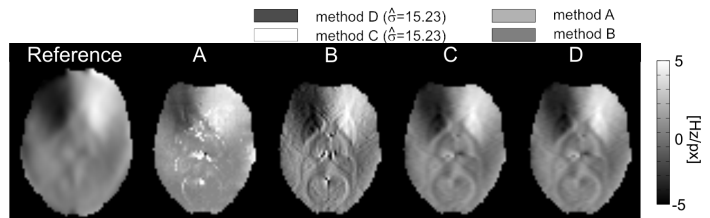


Fig. 3: Reference:  $G_x$  map of the distorted field map (smoothed for visualization). Following are the  $G_x$  maps from the methods A, B, C and D